AMERICAN SOCIETY FOR MICROBIOLOGY | Journal of Bacteriology®

RESEARCH ARTICLE

Rickettsia Lipid A Biosynthesis Utilizes the Late Acyltransferase LpxJ for Secondary Fatty Acid Addition

Mark L. Guillotte,[a] Joseph J. Gillespie,[a] Courtney E. Chandler,[b] M. Sayeedur Rahman,[a] Robert K. Ernst,[b] Abdu F. Azad[a]

[a]Department of Microbiology and Immunology, School of Medicine, University of Maryland, Baltimore, Maryland, USA

[b]Department of Microbial Pathogenesis, School of Dentistry, University of Maryland, Baltimore, Maryland, USA

ABSTRACT Members of the *Rickettsia* genus are obligate intracellular, Gram-negative coccobacilli that infect mammalian and arthropod hosts. Several rickettsial species are human pathogens and are transmitted by blood-feeding arthropods. In Gram-negative parasites, the outer membrane (OM) sits at the nexus of the host-pathogen interaction and is rich in lipopolysaccharide (LPS). The lipid A component of LPS anchors the molecule to the bacterial surface and is an endotoxic agonist of Toll-like receptor 4 (TLR4). Despite the apparent importance of lipid A in maintaining OM integrity, as well as its inflammatory potential during infection, this molecule is poorly characterized in *Rickettsia* pathogens. In this work, we have identified and characterized new members of the recently discovered LpxJ family of lipid A acyltransferases in both *Rickettsia typhi* and *Rickettsia rickettsii*, the etiological agents of murine typhus and Rocky Mountain spotted fever, respectively. Our results demonstrate that these enzymes catalyze the addition of a secondary acyl chain (C_{14}/C_{16}) to the 3′-linked primary acyl chain of the lipid A moiety in the final steps of the Raetz pathway of lipid A biosynthesis. Since lipid A architecture is fundamental to bacterial OM integrity, we believe that rickettsial LpxJ may be important in maintaining membrane dynamics to facilitate molecular interactions at the host-pathogen interface that are required for adhesion and invasion of mammalian cells. This work contributes to our understanding of rickettsial outer membrane physiology and sets a foundation for further exploration of the envelope and its role in pathogenesis.

IMPORTANCE Lipopolysaccharide (LPS) triggers an inflammatory response through the TLR4-MD2 receptor complex and inflammatory caspases, a process mediated by the lipid A moiety of LPS. Species of *Rickettsia* directly engage both extracellular and intracellular immunosurveillance, yet little is known about rickettsial lipid A. Here, we demonstrate that the alternative lipid A acyltransferase, LpxJ, from *Rickettsia typhi* and *R. rickettsii* catalyzes the addition of C_{16} fatty acid chains into the lipid A 3′-linked primary acyl chain, accounting for major structural differences relative to the highly inflammatory lipid A of *Escherichia coli*.

KEYWORDS LPS, lipid A, LpxJ, pathogenesis, *Rickettsia*, outer membrane

Species of *Rickettsia* (*Rickettsiales*: *Alphaproteobacteria*) are Gram-negative obligate intracellular parasites of a vast range of eukaryotes (1). While mechanisms for host cell invasion are variable across rickettsial lineages (2), all rickettsiae lyse the host phagocytic vacuole and reside primarily in the host cytosol (3). Dependent on a plethora of host metabolites, rickettsiae have a diminished metabolic capability relative to that of free-living and facultative intracellular bacteria, as well as vacuolar obligate intracellular species (4). Thus, while rickettsiae vary in their abilities to infect vertebrates and cause pathogenesis, all species are metabolic parasites of the eukaryotic cytoplasm.

Remarkably, despite the lack of glycolytic enzymes, rickettsiae synthesize a typical

Received 12 June 2018 **Accepted** 6 July 2018

Accepted manuscript posted online 16 July 2018

Citation Guillotte ML, Gillespie JJ, Chandler CE, Rahman MS, Ernst RK, Azad AF. 2018. *Rickettsia* lipid A biosynthesis utilizes the late acyltransferase LpxJ for secondary fatty acid addition. J Bacteriol 200:e00334-18. https://doi.org/10.1128/JB.00334-18.

Editor Thomas J. Silhavy, Princeton University

Address correspondence to Abdu F. Azad, aazad@som.umaryland.edu.

Gram-negative bacterial cell envelope (5–7). The inner membrane (IM) and outer membrane (OM) are separated by a relatively thin peptidoglycan layer (8), which contains diaminopimelate in the stem peptide (9). The OM is asymmetric, with the inner leaflet composed mainly of glycerophospholipids (10, 11) and the outer leaflet predominantly composed of lipopolysaccharide (LPS) (12–14). As the interface connecting host to microbe, the rickettsial OM constituents are critically important not only for host cell invasion but also for mediating intracellular survival. The composition of surface proteins has been identified for several species (15–18), and nearly two dozen effectors are recognized as components of the secretome (19); however, the nonproteinaceous surface components of *Rickettsia*, including LPS, are critically understudied.

LPS is highly antigenic in rickettsial infection (20, 21) and is composed of an outer O-antigen polysaccharide linked to a core oligosaccharide, which is anchored in the bacterial outer leaflet by lipid A (22). Lipid A is a pathogen-associated molecular pattern (PAMP) known for its ability to trigger an inflammatory response through its interaction with the Toll-like receptor 4/myeloid differentiation factor 2 (TLR4/MD2) complex, as well as activation of the noncanonical inflammasome through cytosolic caspases (Casp-4/Casp-5 in humans; Casp-11 in mice) (23–25). In a mouse model of rickettsiosis, TLR4/MD2 activation is critical for bacterial clearance (26, 27); however, little is known about the contribution of LPS to the inflammatory nature of *Rickettsia* infection (28, 29). Recent analysis of the lipid A from *Rickettsia typhi* revealed structural differences relative to the highly inflammatory lipid A of *Escherichia coli* though the potential of rickettsial lipid A to act as a TLR4 agonist remains unclear (30) (Fig. 1).

Our recent phylogenomics study indicated that rickettsiae contain a nearly conserved Raetz pathway for the synthesis of lipid A, lacking only the late acyltransferase LpxM (4). LpxM, which catalyzes the 3′ secondary acylation of 3-deoxy-D-*manno*-2-octulosonic acid (KDO_2)-lauroyl-lipid IV_A (typically transferring myristate) subsequent to 2′ secondary acylation (carried out by LpxL), is absent in many bacteria, some of which alternatively carry a nonorthologous late acyltransferase named LpxJ (previously named DUF374) (31–33). LpxJ enzymes of *Helicobacter pylori*, *Campylobacter jejuni*, and *Wolinella succinogenes* (all *Epsilonproteobacteria* pathogens) catalyze 3′ secondary acylation but can or must do so prior to 2′ secondary acylation (LpxL) and even 3-deoxy-D-*manno*-octulosonic acid (KDO) transfer (carried out by the KDO transferase WaaA). Thus, LpxJ enzymes can be considered more functionally promiscuous than their LpxM counterparts. As LpxJ homologs are present in all *Rickettsia* genomes, with the *R. typhi* enzyme sharing 27% identity with *H. pylori* LpxJ, we reasoned that these enzymes complete the Raetz pathway for rickettsial lipid A biosynthesis and incorporate a C_{16} fatty acid chain as a 3′ secondary acylation (30).

Here, we provide enzymatic evidence that *Rickettsia* LpxJ complements *E. coli* LpxM mutants and carries out 3′ secondary acylation of lipid IV_A and lauroyl-lipid IV_A. Additionally, targeted mutagenesis based on comparative analysis of >2,800 DUF374 family members with LpxJ homologs reveals residues critical for acylation. In line with prior work (31), our data demonstrate that divergent LpxJ and LpxM active sites both catalyze 3′ secondary acylation for lipid A biosynthesis and that LpxJ is a nonorthologous replacement of LpxM in a vast range of diverse bacteria. As lipid A architecture is fundamental to OM integrity in Gram-negative bacteria, our findings indicate that LpxJ may be important in maintaining ideal membrane dynamics to facilitate molecular interactions at the host-pathogen interface.

RESULTS

***Rickettsia* encodes a homolog of LpxJ.** Rickettsial comparative genomic analysis has identified a nearly complete Raetz pathway of lipid A biosynthesis (see Fig. S1 in the supplemental material). However, *Rickettsia* species do not encode any enzymes similar to LpxM (also known as MsbB). Since *R. typhi* (and probably all species of *Rickettsia*) produces hexa-acylated lipid A (30), we reasoned that a lipid A acyltransferase analogous to LpxM has escaped gene annotation within rickettsial genomes. In a report describing LpxJ, Rubin et al. identified a putative LpxJ homolog in *R. rickettsii* (27%

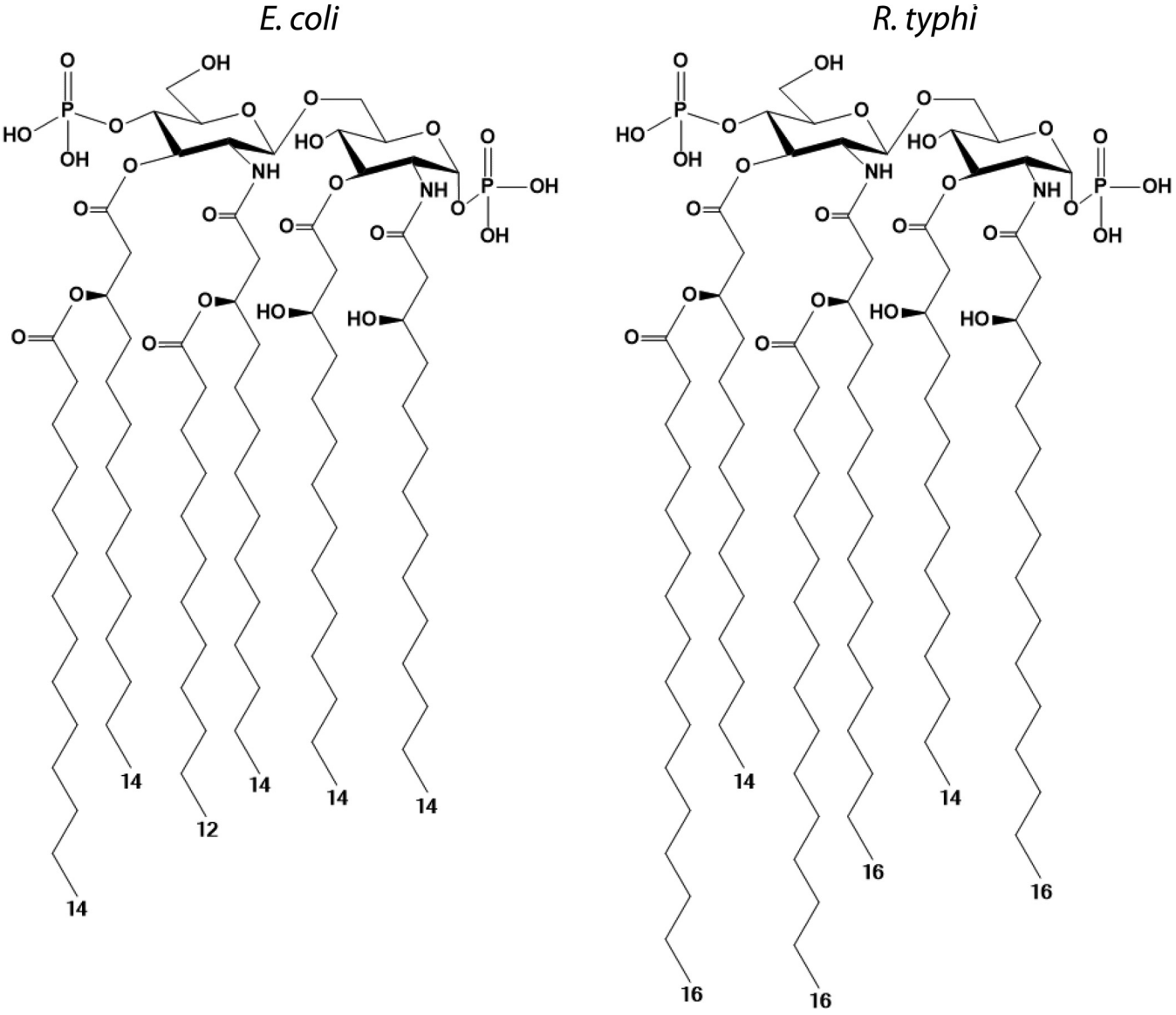

FIG 1 Lipid A structures of *Escherichia coli* and *Rickettsia typhi*.

similarity at the protein level) (31). We have further identified LpxJ family genes throughout the genus *Rickettsia* (Table 1) and have selected putative homologs from *R. typhi* (RT0047) (Fig. S2) and *R. rickettsii* (A1G_00705), here termed LpxJ^{Rt} and LpxJ^{Rr}, respectively, for molecular characterization.

TABLE 1 Conservation between rickettsial LpxJ homologs

Rickettsia species (strain)	Locus tag	Homology[a]		
		% identity	% positive	E value
R. typhi (Wilmington)	RT0047	100	100	2E−161
R. prowazekii (Breinl)	H375_5410	98	99	8E−159
R. rickettsii (Sheila Smith)	A1G_00705	88	92	2E−140
R. felis (LSU)	JS55_00590	89	93	1E−142
R. akari (Hartford)	A1C_00645	85	91	1E−136
R. belli (RML Mogi)	RBEMOGI_1439	79	90	2E−129

[a]BLAST analysis was performed using *R. typhi* (Wilmington) LpxJ primary protein sequence as the query. Zero gaps were found in all query-subject alignments.

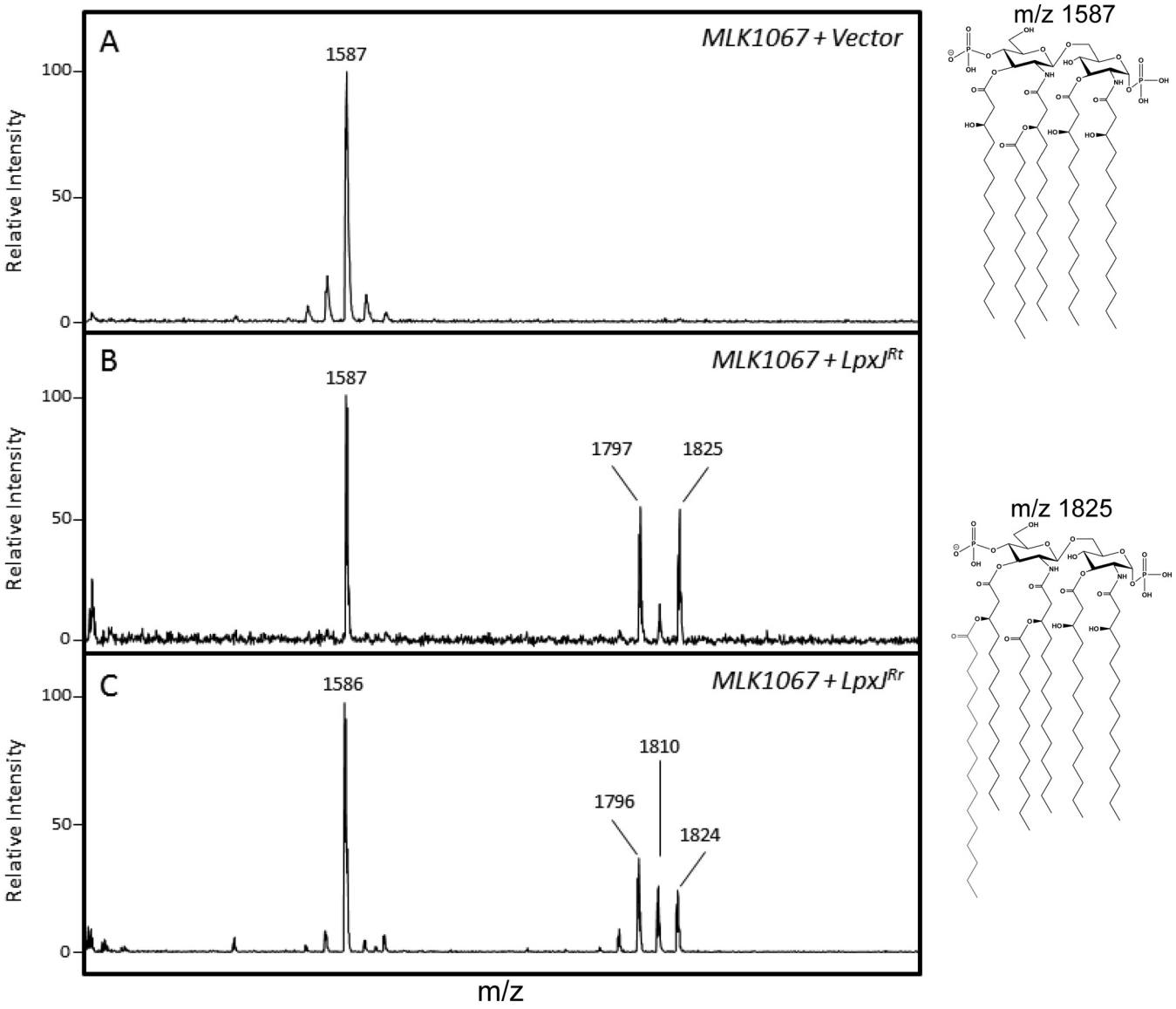

FIG 2 LpxJ^{Rt} and LpxJ^{Rr} complement the loss of LpxM in *E. coli* and restore a hexa-acylated lipid A phenotype. (A) *E. coli* mutant strain MLK1067 (Δ*lpxM*) produces mostly penta-acylated lipid A, corresponding to a major ion peak at *m/z* 1,587. (B and C) Expression of LpxJ^{Rt} (B) or LpxJ^{Rr} (C) restores a hexa-acylated lipid A phenotype by addition of C_{14} or C_{16} fatty acid corresponding to the molecular ion at *m/z* 1,797 or *m/z* 1,825, respectively.

LpxJ^{Rt} and LpxJ^{Rr} complement an *E. coli* LpxM mutant. In order to investigate the role of LpxJ in *Rickettsia* lipid A biosynthesis, we utilized a heterologous system in which acylation-deficient lipid A mutants of *E. coli* act as a reporter of enzyme function for exogenously expressed acyltransferases. We first expressed LpxJ^{Rt} and LpxJ^{Rr} in the *lpxM* mutant MLK1067 that elaborates predominately penta-acylated lipid A. After expression of rickettsial proteins was induced (Fig. S3), lipid A extractions were prepared and subjected to matrix-assisted laser desorption ionization–time of flight mass spectrometry (MALDI-TOF MS) analysis to determine if rickettsial LpxJ can complement the loss of *lpxM* and produce hexa-acyl lipid A. In comparison to results in untransformed MLK1067, we observed additional lipid A species of increased mass from cells expressing LpxJ^{Rt} and LpxJ^{Rr} but no change from cultures transformed with an empty plasmid vector (Fig. 2). The ions at *m/z* 1,797 and *m/z* 1,825 represent the addition of C_{14} (Δ*m/z* 210) or C_{16} (Δ*m/z* 238), respectively, to the parental penta-acylated lipid A (*m/z* 1,587). MALDI-TOF MS results for LpxJ^{Rt} were confirmed using gas chromatography (GC). Fatty acid peaks were identified by comparison to commercially available

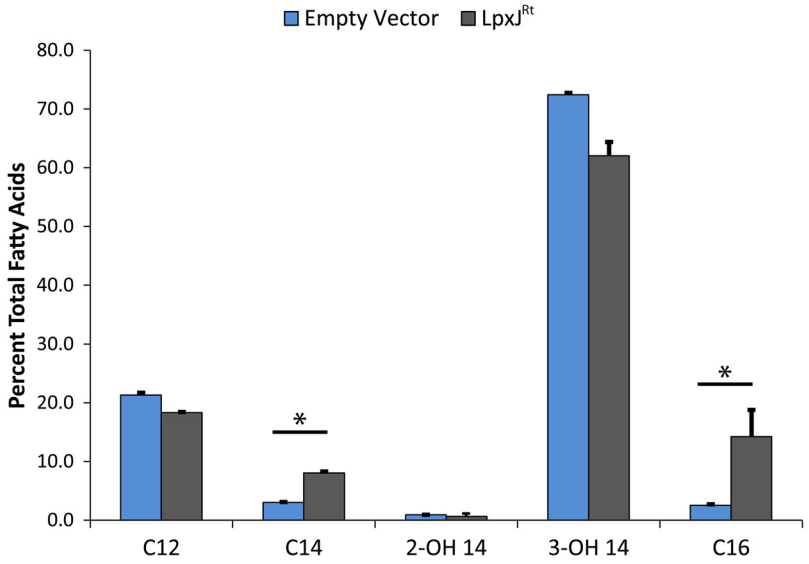

FIG 3 LpxJ transfers secondary C_{14} or C_{16} to the hydroxymyristate at the 3′ position. The fatty acid proportions present in the LPS isolated from *E. coli* strain MLK1067 carrying an empty vector or expressing *lpxJ* of *R. typhi* are given as percentages of the total identified fatty acids. A 4-fold increase of C_{14} and C_{16} addition was observed in the *E. coli* mutant complemented with *lpxJ*^{Rt}. Analysis was run in biological triplicate from three isolated transformants and values were plotted ± standard deviations. *, $P < 0.05$, as determined by Student's *t* test.

bacterial acid methyl ester (BAME) standards. The amount of each fatty acid present in lipid A was calculated by comparison to an internal pentadecanoic acid (C_{15}) standard over three biological replicates. LpxJ^{Rt}-overexpressing cells show a 4-fold increase in the total amount of C_{14} and C_{16} (Fig. 3). Taken together, these data indicate that LpxJ^{Rt} and LpxJ^{Rr} are bona fide acyltransferases in the lipid A pathway.

LpxJ^{Rt} activity is independent of LpxL activity. In *E. coli* lipid A synthesis, the final fatty acid addition by LpxM requires the prior activity of LpxL, the 2′ secondary acyltransferase (KDO_2-lauroyl-lipid IV_A substrate) (34). In contrast to LpxM's rigid substrate selection, LpxJ has flexibility in its activity. LpxJ of *H. pylori* can act independently of LpxL activity, while homologs from *C. jejuni* and *W. succinogenes* act exclusively on tetra-acylated substrates. LpxJ^{Rt} is shown above to act upon penta-acylated lipid A molecules (Fig. 2), but it is unclear whether this is the only lipid A precursor that is a substrate. To determine the requirement of LpxL activity on the activity of LpxJ, we expressed LpxJ in *E. coli* strain MKV15b (35), which produces mostly tetra-acylated lipid A lacking secondary acylation on the 2′ and 3′ fatty acids (Fig. 4). We found that LpxJ^{Rt} acts upon tetra-acylated substrate (*m/z* 1,404), transferring C_{14} or C_{16} fatty acids (*m/z* 1,615 and 1,642, respectively). These data suggest that *Rickettsia* lipid A synthesis does not share the strict operational order of acyl chain incorporation found in *E. coli*.

Global analysis reveals conserved LpxJ residues critical for acyl transfer. Analysis of 2,842 distinct LpxJ homologs identified four conserved regions (Fig. 5A). Interestingly, none of these regions contained an HX_4D/E motif, the hallmark acid/base catalytic mechanism, or charge relay system, that defines glycerol-3-phosphate acyltransferase (GPAT), lysophosphatidic acid acyltransferase (LPAAT), dihydroxyacetonephosphate acyltransferase (DHAPAT), and 2-acyl-glycerophosphoethanolamine acyltransferase (LPEAT) (36). To gain insight on residues possibly comprising an alternative charge relay system in the LpxJ^{Rt} active site, we mutated conserved His [H61A and H84(A/S)] and Asp (D86A, D132A, and D173A) residues within these regions, as well as two highly conserved Trp residues (W60A and W172A). Aside from H84(A/S), these mutants lacked the enzymatic function of LpxJ^{Rt} when expressed in MLK1067, reverting the lipid A phenotype to that of the background strain (penta-acyl, *m/z* 1,587) (Fig. 5B). The negligible effect on LpxJ^{Rt} activity observed by mutating H84 to either Ala or Ser (data not shown) indicates that H61 is the likely catalytic base of LpxJ.

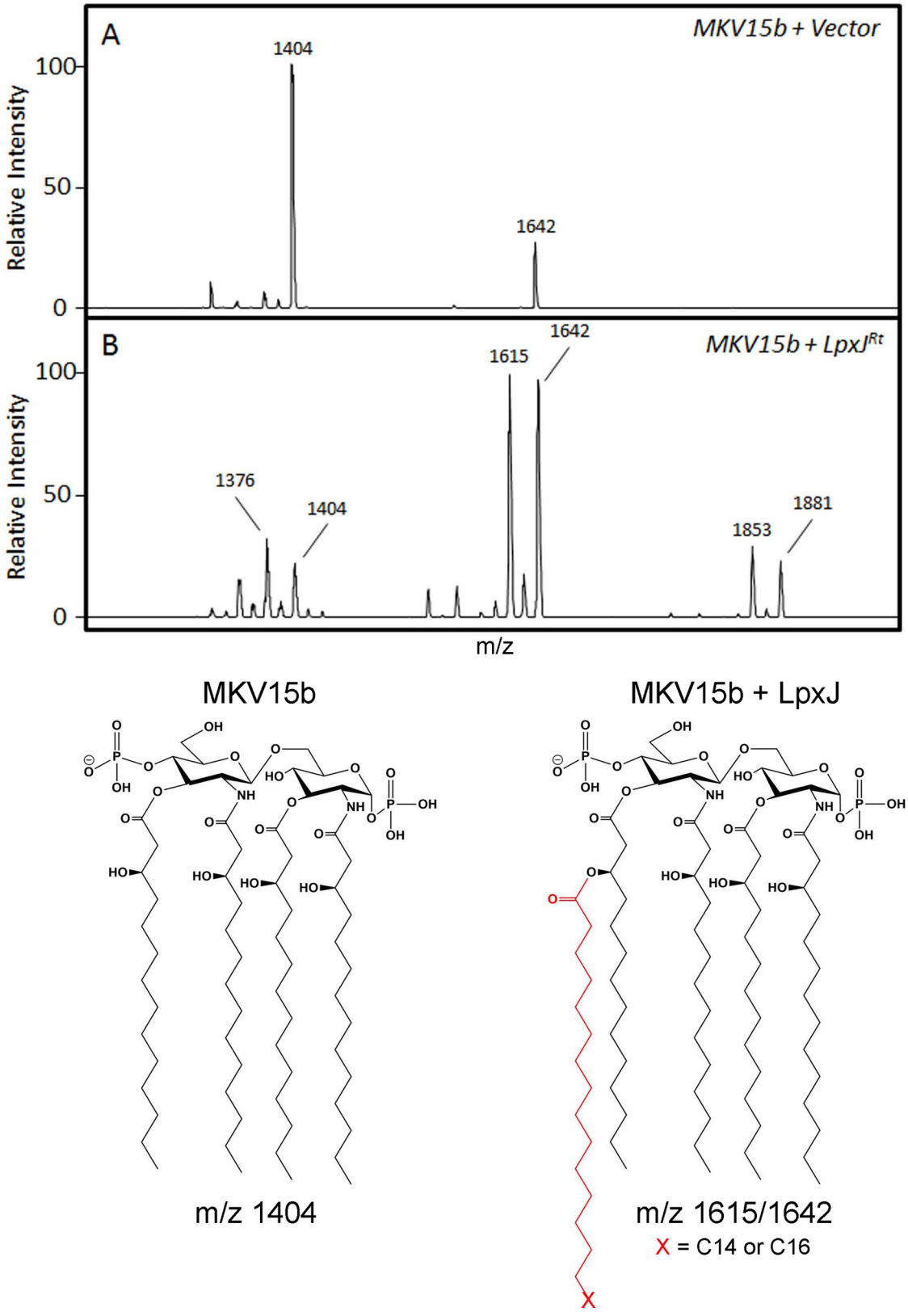

FIG 4 Acylation of lipid A by LpxJ^{Rt} does not depend upon prior secondary acylation. MALDI-TOF MS analysis was performed of lipid A from *E. coli* strain MKV15b (Δ*lpxM* Δ*lpxL* Δ*lpxP*) (35) transformed with empty vector (A) or expressing LpxJ^{Rt} (B). The tetra-acylated major lipid A ion of the parental strain (*m/z* 1,404) is acylated by LpxJ, which catalyzes the addition of C_{14} (*m/z* 1,614) or C_{16} (*m/z* 1,642). The minor ion peak at *m/z* 1,642 shown in panel A is likely the result of minimal constitutive PagP activity in this strain. A complete list of peaks and their raw measurements are reported in Table S1 in the supplemental material.

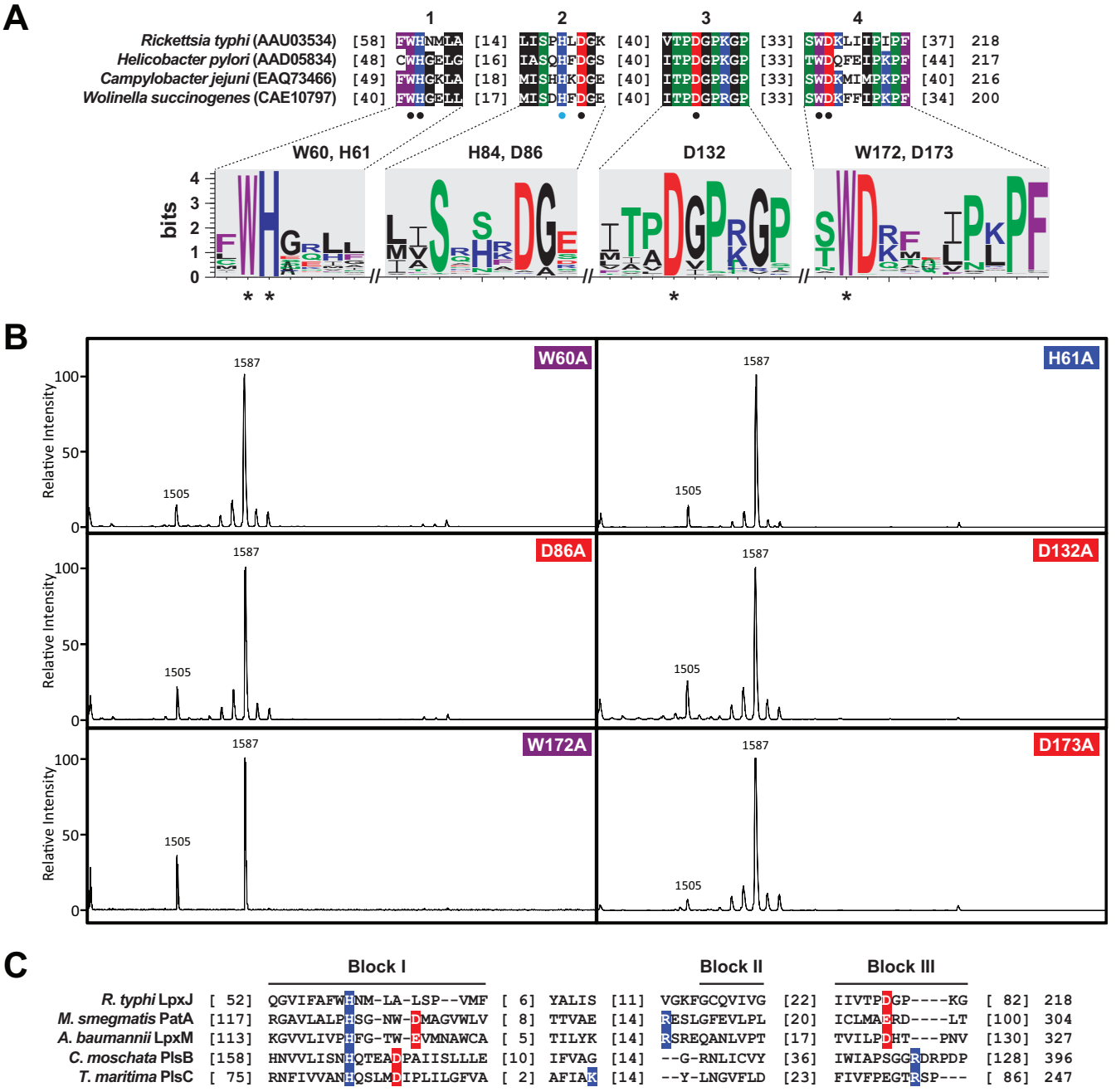

FIG 5 Structural and mutational analysis of LpxJ homologs. (A) Multiple sequence alignment of *Rickettsia typhi* LpxJ and three *Epsilonproteobacteria* LpxJ homologs that were previously characterized as lipid A late acyltransferases (31). NCBI protein accession numbers are in parentheses. Only the four most conserved regions of the alignment are shown (numbered 1 to 4 above the sequences). Amino acid coloring is as follows: black, hydrophobic; red, negatively charged; green, hydrophilic; purple, aromatic; blue, positively charged. Black and light blue circles below indicate critical and noncritical residues, respectively, as determined by mutagenesis, shown in panel B. Below each conserved region is a sequence logo (57) depicting conservation across 2,842 compiled LpxJ homologs. Asterisks denote the four residues invariant across all LpxJ homologs. (B) The histidine, aspartic acid, or tryptophan residue at the indicated position in the primary sequence of LpxJ was mutated to alanine, and each construct was individually expressed in MLK1067. Loss of these highly conserved residues abolished the acyltransferase activity of the enzyme, reverting the lipid A phenotype to that of the background strain (penta-acyl, *m/z* 1,587). Mutation of histidine at position 84 to alanine or serine had no effect on enzymatic activity (data not shown). (C) Comparison of *R. typhi* LpxJ to four divergent lipid acyltransferases. Proteins with associated structures were obtained from the Protein Data Bank: *Mycobacterium smegmatis* PatA (PDB code 5F34), *Acinetobacter baumannii* LpxM (5KNK), *Cucurbita moschata* PlsB (1IUQ), and *Thermotoga maritima* PlsC (5KYM). *R. typhi* LpxJ was modeled to all four acyltransferase structures using Phyre2 (58) and fitted to an existing structural alignment template (37), which follows the convention established for naming conserved blocks within GPAT, LPAAT, DHAPAT, and LPEAT acyltransferases (59, 60). Active-site residues for each structure are colored. For LpxJ, Asp132 is proposed to participate in the active site charge relay system with His61 (36, 61).

Provided that all three Asp mutants abolished LpxJ activity, we compared LpxJ to four divergent lipid acyltransferases for which structures have been solved (Fig. 5C). Modeling LpxJ^{Rt} (RT0047) to these structures consistently positioned H61 within the canonical charge relay system (block I). Fitting LpxJ^{Rt} to a structural alignment template (37) positioned D132 with other negatively charged residues in PatA (block III). This suggests that LpxJ is similar to lipid acyltransferases, which have diverged from the canonical HX_4(D/E) motif by completing the charge relay system across blocks I and III (Fig. 5C). Unlike PatA, however, LpxJ does not have a second positively charged residue (block II) coordinating in the active site, which likely explains the lack of a conserved Asp or Glu within block I for LpxJ. This indicates further divergence of its charge relay system and distinguishes LpxJ from any known lipid acyltransferase.

DISCUSSION

Rickettsia species are obligate intracellular bacterial parasites that produce a typical Gram-negative envelope with the IM and OM separated by a thin peptidoglycan layer (4, 5). Considering the invasive lifestyle of these parasites, the OM sits at the nexus of the host-pathogen interface and is rich in LPS, the classical Gram-negative PAMP (24). Understanding the interplay between mammalian and bacterial molecules at the host-pathogen interface is critically important for the development of novel therapeutic approaches. Considering the historical role of LPS as a mediator of inflammation and its location at the front line of host-pathogen interactions, it is safe to assume that LPS plays a role during *Rickettsia* infection. However, despite the apparent importance of LPS, there exists a paucity of information about the biology of LPS biosynthesis and its contribution to virulence. In order to address this gap in our understanding of this molecule, we have begun foundational work elucidating the basics of LPS biogenesis in *Rickettsia*. Here, we characterize new members of the recently discovered LpxJ family of lipid A acyltransferases from *R. typhi* and *R. rickettsii*. Using an *E. coli* reporter system, we have identified LpxJ^{Rt} and LpxJ^{Rr} to be lipid A acyltransferases in *Rickettsia*. These enzymes catalyze the transfer of secondary fatty acids, predominately C_{14} or C_{16}, to the 3-hydroxyl group of the 3′ primary acyl chain. Interestingly, LpxJ^{Rt} shows no preference for either penta- or tetra-acylated lipid A in our reporter system. This implies that activity of the enzyme is bispecific for either lipid IV_A or acyl-lipid IV_A and can act before LpxL (RT0704), similar to the previously characterized LpxJ homolog from *H. pylori*. These data indicate that multiple paths exist for secondary acylation of *Rickettsia* lipid A (Fig. 6) and that secondary fatty acid diversity can be more extensive than described by Fodorová et al. (30). Our analysis of *R. typhi* lipid A shown in Fig. S4 in the supplemental material indicates a minor lipid A peak at *m/z* 1,907 that is characteristic of shorter fatty acid chain incorporation than that of the major peak at *m/z* 1,936 depicted in Fig. 1. It is conceivable that the C_{14}/C_{16} promiscuity observed for LpxJ activity can be contributing to this *in vivo* heterogeneity. Further, both LpxJ homologs characterized here catalyze the addition of fatty acids with odd chain lengths, represented by the peak at *m/z* 1,810 in Fig. 2A and B. This addition is likely an artifact as neither *E. coli* nor *Rickettsia* spp. naturally produce odd chain fatty acids (4, 38). It is possible that the presence of short-chain fatty acid metabolites in the growth medium causes nonnatural fatty acid synthesis leading up to cell lysis, as *E. coli* does produce some odd-chain-length fatty acids when grown in the presence of propionic acid (39). It is also possible that overexpression of rickettsial LpxJ in a heterologous *E. coli* system is influencing fatty acid biosynthesis and causing erroneous incorporation of odd-length, short-chain fatty acids as building blocks instead of the typical condensation of malonyl-coenzyme A (CoA) during fatty acid manufacturing.

The requirement for Kdosylation of lipid IV_A prior to LpxJ^{Rt} activity was not tested here. The *E. coli* pathway requires KDO sugars be present on lipid IV_A prior to secondary acylation by LpxL and LpxM (40). However, previously characterized LpxJ homologs did not share this requirement (31). The combination of fatty acid selection (C_{14}-C_{16}) and substrate promiscuity (tetra/penta-acyl lipid IV_A) is unique in comparison to the three

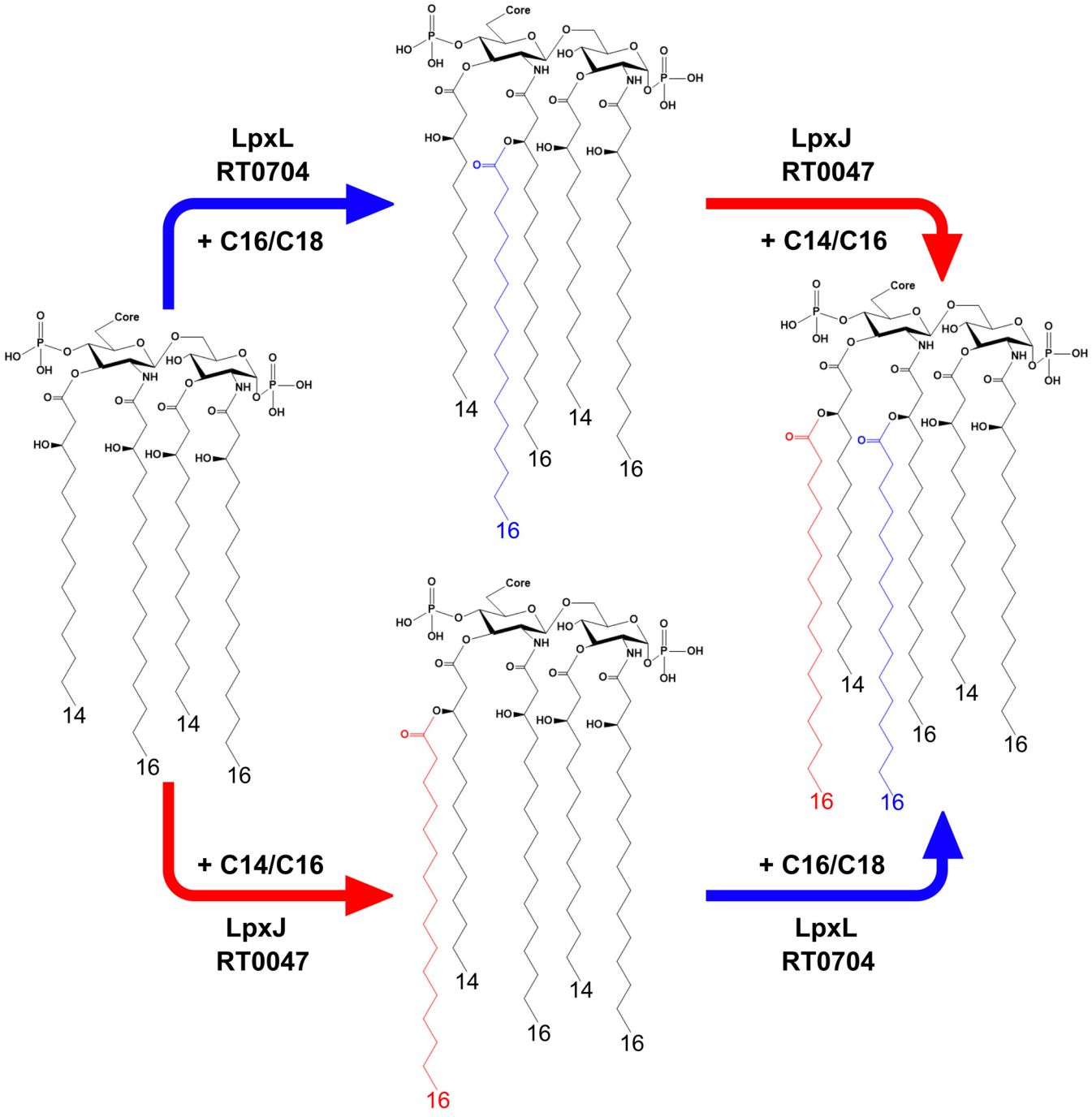

FIG 6 Late acyltransferase activity for *R. typhi*. The bidirectional additions of the final two fatty acids to complete the biosynthesis of lipid A at the conclusion of the Raetz pathway are shown. Blue arrows indicate LpxJ-mediated acylation, and red arrows indicate LpxL-mediated acylation.

previously characterized LpxJ homologs, further expanding the diversity of LpxJ family acyltransferase activity.

Our comparative genomics analysis indicates that LpxJ homologs (all members of DUF374) are widespread across *Bacteria* (Fig. 5A). These enzymes have functions analogous to the function of the canonical LpxM acyltransferase, and their discovery fills a long-standing hole in the Raetz pathway of lipid A biosynthesis in LpxM-deficient bacteria. Indeed, *in silico* structural prediction of LpxJ^{Rt} indicates superficial similarities across LpxJ and PatA, a recently crystallized member of the LPLAT superfamily that contains an active site deviating from sites of canonical lipid acyltransferases (Fig. 5C).

TABLE 2 *E. coli* strains used in this study

Strain	Genotype or description	Reference or source
MKV15b	Δ*lpx*M Δ*lpx*L Δ*lpx*P	35
MLK1067 (CGSC 7701)[a]	λ⁻ *lpxM11*(Ω)::Cm IN(*rrnD-rrnE*)*1 rph-1*	34
MLK+LpxJ	MLK1067 transformed with pFLAG vector carrying RT0047 (LpxJ^{Rt}) or A1G_00705 (LpxJ^{Rr})	This work
MLK+JH61A	MLK+LpxJ^{Rt} with His61 mutated to alanine	This work
MLK+JH84A	MLK+LpxJ^{Rt} with His84 mutated to alanine	This work
MLK+JW60A	MLK+LpxJ^{Rt} with Trp60 mutated to alanine	This work
MLK+JD86A	MLK+LpxJ^{Rt} with Asp86 mutated to alanine	This work
MLK+JD132A	MLK+LpxJ^{Rt} with Asp132 mutated to alanine	This work
MLK+JW172A	MLK+LpxJ^{Rt} with Trp172 mutated to alanine	This work
MLK+JD173A	MLK+LpxJ^{Rt} with Asp173 mutated to alanine	This work

[a]CGSC, Cole Genetic Stock Center, Yale University.

Further, we identified six highly conserved residues in all LpxJ homologs, which we confirmed were necessary for LpxJ function (Fig. 5A and B). These include a histidine at position 61 and an aspartate at position 132 that we believe represent an active-site catalytic dyad similar to PatA. Although these amino acids are distant in the primary sequence, structural modeling predicts a close spatial arrangement of these two residues (37, 41) (Fig. 5C). It is likely that these residues are positioned sufficiently close to allow charge interactions, abstracting a proton from the acceptor hydroxyl and facilitating nucleophilic attack of the incoming acyl chain thioester bond. This putative charge relay system is supported by the recently published crystal structures of PatA from *Mycobacterium smegmatis* (37, 41), which does not contain the classical HX_4D motif that is found in other lipid A acyltransferases (42–44) but is absent in LpxJ. Based on the conservation of the proposed catalytic residues within DUF374-containing acyltransferases, this active-site orientation might be common within the LpxJ family.

Lipid A architecture is fundamental to bacterial OM integrity. In many Gram-negative pathogens, changes in lipid A structure can have a profound impact on virulence (45, 46). Therefore, we infer that *Rickettsia* LpxJ is also important in maintaining ideal membrane dynamics and facilitating molecular interactions at the host-pathogen interface that are required for adhesion and invasion of mammalian cells. Additionally, lipid A is the endotoxic component of LPS (47), and activation of TLR4 is critical for bacterial clearance in mouse models of *Rickettsia* infection (27, 48), as well as other intracellular parasites (49–51). These data, as well as a recent report highlighting host-specific differences in lipid A gene expression (52), suggest a role for LpxJ in *Rickettsia* virulence, making this enzyme a tempting target for mutational studies *in vivo*. Further work promises to reveal novel insights into *Rickettsia* pathogenesis and contribute greatly to our understanding of rickettsial OM physiology.

MATERIALS AND METHODS

Recombinant DNA techniques, bacterial strains, and growth conditions. Primers used in this study were obtained from Integrated DNA Technologies (IDT) and are listed in Table 2. Genomic DNA was isolated from *R. typhi* grown in Vero76 tissue monolayer as previously described (53). *lpxJ*^{Rt} (RT0047; NCBI accession number AAU03534) was amplified using Q5 polymerase 2× master mix (M0492; NEB) and gel purified (740609.50; Macherey-Nagel) before infusion cloning (639649; Clontech) into a *lac*-inducible pFLAG-ctc vector (discontinued; Sigma) using HindIII and XhoI restriction sites. Expression of rickettsial genes after induction was verified by immunoblot detection of the C-terminal FLAG epitope tag. *E. coli* cultures in mid-log growth phase were induced with 0.5 mM isopropyl-β-D-thiogalactopyranoside (IPTG) for 90 min at 42°C with shaking (225 rpm). Induced cultures and uninduced control cultures were harvested by centrifugation at 4,895 × *g* for 15 min and suspended in 1× NuPAGE Bolt sample buffer containing 1× NuPAGE reducing agent at a concentration of 100 μl of sample buffer for every 1 ml of culture. Samples were heated to 70°C for 10 min and sonicated briefly to fragment genomic DNA. Proteins were separated by SDS-PAGE and transferred to polyvinylidene difluoride (PVDF) membranes, where recombinant LpxJ proteins were detected by indirect chemiluminescent immunoblot analysis using anti-FLAG (F1804; Sigma) primary antibody at a 1:5,000 dilution, followed by goat anti-mouse horseradish peroxidase (HRP)-conjugated secondary antibody (405306; BioLegend) (see Fig. S3 in the supplemental material). The resulting constructs are designated pFLAG-*lpxJ*^{Rt} and pFLAG-*lpxJ*^{Rr}. Site-directed mutagenesis reactions of selected residues within pFLAG-*lpxJ*^{Rt} were carried out using a QuikChange Lightning kit (210519; Agilent). Primers for mutagenesis are listed in Table 2, and protein expression was verified as described above.

TABLE 3 Primers used in this study

Primer application and name[a]	Primer sequence (5′→3′)[b]
Cloning	
LpxJ_to_pFLAG.Fw	ATATCATATGAAGCTTATGCGAAAAGCTCTTAAAAAATTTTTAAAAAATAGTAAATGCT
LpxJ_to_pFLAG.Rv	CCCGGGAATTCTCGA**CC**TTTCTTTAAGCTCTCTGTTAAGCTTTTTAATTGT
SDM	
SiteMut_H61toA_top	GGTGTAATCTTTGCATTTTGG**GC**TAATATGCTTGCCTTAAGTCCC
SiteMut_H61toA_bottom	GGGACTTAAGGCAAGCATATTA**GC**CCAAAATGCAAAGATTACACC
SiteMut_H84toA_top	ATCTATGCTTTAATATCACCA**GC**TTTAGATGGTAAAATTTTAAAC
SiteMut_H84toA_bottom	GTTTAAAATTTTACCATCTAAA**GC**TGGTGATATTAAAGCATAGAT
SiteMut_D86toA_top	TATCTATGCTTTAATATCACCACATTTAG**C**TGGTAAAATTTTAAACGCCATAGTAGGGA
SiteMut_D86toA_bottom	TCCCTACTATGGCGTTTAAAATTTTACCA**G**CTAAATGTGGTGATATTAAAGCATAGATA
SiteMut_D132toA_top	CAAGGTGCAAATATAATAGTTACACCGG**C**TGGTCCTAAAGGACCTGTATATAAAGTAAA
SiteMut_D132toA_bottom	TTTACTTTATATACAGGTCCTTTAGGACCA**G**CCGGTGTAACTATTATATTTGCACCTTG
SiteMut_D173toA_top	CTTCTAGGTATTTCAGATTAAAAAGTTGGG**C**TAAATTAATAATACCAATACCGTTTGGT
SiteMut_D173toA_bottom	ACCAAACGGTATTGGTATTATTAATTTA**G**CCCAACTTTTTAATCTGAAATACCTAGAAG
SiteMut_W60toA_top	AAATGAACAAGGTGTAATCTTTGCATTT**GC**GCATAATATGCTTGCCTTAAGTCCCGTTA
SiteMut_W60toA_bottom	ATAACGGGACTTAAGGCAAGCATATTATGC**GC**AAATGCAAAGATTACACCTTGTTCATTT
SiteMut_W172toA_top	TACTTCTAGGTATTTCAGATTAAAAAGT**GC**GGATAAATTAATAATACCAATACCGTTTG

[a]SDM, site-directed mutagenesis.
[b]Boldface letters represent nucleotides changed in site-directed mutagenesis.

Bacterial strains used in this study are listed in Table 3. From frozen stocks, *E. coli* was diluted 1:100 after overnight growth into LB broth supplemented with 1 mM magnesium and containing the appropriate antibiotics. Diluted cultures were then grown with shaking (225 rpm) at 37°C to mid-log phase. Protein expression was induced by addition of IPTG to a final concentration of 1 mM. Induction was carried out at 42°C with shaking (60 rpm) for 90 min. Whole cultures were harvested by centrifugation at 5,000 rpm for 10 min, the supernatants were discarded, and the pellets were either snap-frozen in liquid nitrogen before lipid A microextraction or lyophilized prior to fatty acid analysis.

Lipid A microextraction. Microextraction of lipid A from *E. coli* cultures was performed as previously described (54, 55). Briefly, pellets from 5 ml of mid-log phase *E. coli*, grown and induced as described above, were extracted in 400 μl of a solution containing five parts of isobutyric acid and three parts of 1 M ammonium hydroxide and heated at 100°C for 1 h, followed by a 15-min incubation on ice and centrifugation at 2,000 $\times$ *g* for 15 min. Supernatant was collected and mixed in equal parts with water and then frozen and lyophilized. Contaminants were washed from the dried material by two rounds of methanol washes using 1 ml of methanol, followed by sonication and pelleting at 10,000 $\times$ *g* for 5 min. The final product was reconstituted in 2:1:0.25 chloroform-methanol-water (50 μl) along with 4 to 8 grains of Dowex ion exchange resin (Fisher Scientific, Pittsburgh, PA) and incubated with vortexing for at least 5 min. Solubilized lipid A molecules (1 to 2 μl) were spotted onto a stainless steel target plate along with 1 μl of Norharmane matrix (10 mg/ml in 2:1 chloroform-methanol) for MALDI analysis on a Bruker MicroFlex matrix-assisted laser desorption ionization–time of flight (MALDI-TOF) mass spectrometry instrument in negative-ion mode calibrated with Agilent tuning mix (G2421A; Santa Clara, CA), and data were processed using flexAnalysis software (Bruker Daltonics). All microextraction chemicals were obtained from Sigma-Aldrich unless otherwise noted.

GC fatty acid analysis. LPS fatty acids were converted to fatty acid methyl esters (FAMEs) and analyzed using gas chromatography flame ionization detection (GC-FID) as previously described (56). Briefly, lyophilized bacterial cell pellets from 50-ml cultures prepared as described above were incubated at 70°C for 1 h in 500 μl of 90% phenol and 500 μl of water. Samples were then cooled on ice for 5 min and centrifuged at 9,391 $\times$ *g* for 10 min. The aqueous layer was collected, and 500 μl of water was added to the lower (organic) layer and incubated again. This process was repeated two additional times, and all aqueous layers were pooled. Two milliliters of diethyl ether (E-138-1; Fisher) was added to the harvested aqueous layers. This mixture was then vortexed and centrifuged at 2,095 $\times$ *g* for 5 min. The upper (organic) phase was then aspirated off, and 2 ml of diethyl ether was added back to the remaining aqueous phase. The mixture was vortexed and centrifuged at 2,095 $\times$ *g* for 5 min, and the lower (aqueous) phase was collected and then frozen and lyophilized overnight. LPS fatty acids were converted to fatty methyl esters in the presence of 10 μg of pentadecanoic acid (P-6125; Sigma) as an internal standard, using 200 μl of 2 M methanolic HCl (Alltech, Lexington, KY) at 90°C for 18 h. Samples were cooled to room temperature, and 200 μl of NaCl-saturated water was added. Converted fatty methyl esters were then extracted twice with hexane and run on an HP 5890 series 2 gas chromatograph. Retention times were correlated to fatty acids using GC-BAME standards (1114; Matreya, Pleasant Gap, PA).

***In silico* analysis.** To evaluate *Rickettsia typhi* RT0047 (NCBI locus tag AAU03534) as an LpxJ homolog, we aligned it with previously characterized LpxJ proteins: *Helicobacter pylori* (AAD05834), *Campylobacter jejuni* (EAQ73466), and *Wolinella succinogenes* (CAE10797). To further assess conserved regions of LpxJ proteins, we retrieved 2,842 putative homologs from the NCBI nonredundant protein database in blastp searches using RT0047 as the query. Proteins were aligned, with four conserved regions further evaluated for conservation using WebLogo (57). Both above-mentioned multiple sequence alignments were

constructed using MUSCLE (31) (default parameters). Finally, we compared RT0047 to four divergent lipid acyltransferases that have associated structures: *Mycobacterium smegmatis* PatA (PDB accession number 5F34), *Acinetobacter baumannii* LpxM (PDB accession number 5KNK), *Cucurbita moschata* PlsB (PDB accession number 1IUQ), and *Thermotoga maritima* PlsC (PDB accession number 5KYM). *R. typhi* LpxJ was modeled to all four acyltransferase structures using Phyre2 (58) and fitted to an existing structural alignment template (37), which follows the convention established for naming conserved blocks within GPAT, LPAAT, DHAPAT, and LPEAT acyltransferases (59, 60).

SUPPLEMENTAL MATERIAL

Supplemental material for this article may be found at https://doi.org/10.1128/JB.00334-18.

SUPPLEMENTAL FILE 1, PDF file, 0.6 MB.

ACKNOWLEDGMENTS

We acknowledge Francesca Gardner, Kelsey Gregg, Erin Harberts, Belita Opene, Alison Scott, and Magda Beier-Sexton for their support.

This work was supported with funds from National Institutes of Health/National Institute of Allergy and Infectious Diseases grants (R01AI017828 and R01AI126853 to A.F.A., R21AI26108 to J.J.G. and M.S.R., and R01AI123820 to R.K.E.). M.L.G. was supported in part by NIH/NIAID grant T32AI095190 (Signaling Pathways in Innate Immunity).

The content is solely the responsibility of the authors and does not necessarily represent the official views of the funding agencies. The funders had no role in study design, data collection and analysis, decision to publish, or preparation of the manuscript.

REFERENCES

1. Gillespie JJ, Nordberg EK, Azad AF, Sobral BWS. 2012. Phylogeny and comparative genomics: the shifting landscape in the genomics era, p 84–141. *In* Palmer GH, Azad AF (ed), Intracellular pathogens II: rickettsiales. ASM Press, Washington, DC.
2. Rennoll-Bankert KE, Rahman MS, Gillespie JJ, Guillotte ML, Kaur SJ, Lehman SS, Beier-Sexton M, Azad AF. 2015. Which way in? The RalF Arf-GEF orchestrates *Rickettsia* host cell invasion. PLoS Pathog 11:e1005115. https://doi.org/10.1371/journal.ppat.1005115.
3. Winkler HH. 1986. Early events in the interaction of the obligate intracytoplasmic parasite, Rickettsia prowazekii, with eucaryotic cells: entry and lysis. Ann Inst Pasteur Microbiol 137A:333–336.
4. Driscoll TP, Verhoeve VI, Guillotte ML, Lehman SS, Rennoll SA, Beier-Sexton M, Rahman MS, Azad AF, Gillespie JJ. 2017. Wholly *Rickettsia*! Reconstructed metabolic profile of the quintessential bacterial parasite of eukaryotic cells. mBio 8:e00859-17. https://doi.org/10.1128/mBio.00859-17.
5. Smith DK, Winkler HH. 1979. Separation of inner and outer membranes of Rickettsia prowazeki and characterization of their polypeptide compositions. J Bacteriol 137:963–971.
6. Peturova M, Vitiazeva V, Toman R. 2015. Structural features of the O-antigen of Rickettsia typhi, the etiological agent of endemic typhus. Acta Virol 59:228–233. https://doi.org/10.4149/av_2015_03_228.
7. Amano KI, Williams JC, Dasch GA. 1998. Structural properties of lipopolysaccharides from Rickettsia typhi and Rickettsia prowazekii and their chemical similarity to the lipopolysaccharide from Proteus vulgaris OX19 used in the Weil-Felix test. Infect Immun 66:923–926.
8. Silhavy TJ, Kahne D, Walker S. 2010. The bacterial cell envelope. Cold Spring Harb Perspect Biol 2:a000414. https://doi.org/10.1101/cshperspect.a000414.
9. Pang H, Winkler HH. 1994. Analysis of the peptidoglycan of Rickettsia prowazekii. J Bacteriol 176:923–926. https://doi.org/10.1128/jb.176.3.923-926.1994.
10. Tzianabos T, Moss CW, McDade JE. 1981. Fatty acid composition of rickettsiae. J Clin Microbiol 13:603–605.
11. Winkler HH, Miller ET. 1978. Phospholipid composition of Rickettsia prowazeki grown in chicken embryo yolk sacs. J Bacteriol 136:175–178.
12. Schramek S, Brezina R, Kazár J. 1977. Some biological properties of an endotoxic lipopolysaccharide from the typhus group rickettsiae. Acta Virol 21:439–441.
13. Fumarola D, Munno I, Monno R, Miragliotta G. 1980. Lipopolysaccharides from Rickettsiaceae: limulus endotoxin assay and pathogenetic mediators in rickettsiosis. Acta Virol 24:155.
14. Fumarola D, Munno I, Monno R, Miragliotta G. 1979. Lipopolysaccharides of Rickettsiaceae and the Limulus endotoxin assay. G Batteriol Virol Immunol 72:40–43. (In Italian.)
15. Pornwiroon W, Bourchookarn A, Paddock CD, Macaluso KR. 2009. Proteomic analysis of Rickettsia parkeri strain Portsmouth. Infect Immun 77:5262–5271. https://doi.org/10.1128/IAI.00911-09.
16. Sears KT, Ceraul SM, Gillespie JJ, Allen ED, Popov VL, Ammerman NC, Rahman MS, Azad AF. 2012. Surface proteome analysis and characterization of surface cell antigen (Sca) or autotransporter family of Rickettsia typhi. PLoS Pathog 8:e1002856. https://doi.org/10.1371/journal.ppat.1002856.
17. Qi Y, Xiong X, Wang X, Duan C, Jia Y, Jiao J, Gong W, Wen B. 2013. Proteome analysis and serological characterization of surface-exposed proteins of Rickettsia heilongjiangensis. PLoS One 8:e70440. https://doi.org/10.1371/journal.pone.0070440.
18. Renesto P, Samson L, Ogata H, Azza S, Fourquet P, Gorvel JP, Heinzen RA, Raoult D. 2006. Identification of two putative rickettsial adhesins by proteomic analysis. Res Microbiol 157:605–612. https://doi.org/10.1016/j.resmic.2006.02.002.
19. Gillespie JJ, Kaur SJ, Rahman MS, Rennoll-Bankert K, Sears KT, Beier-Sexton M, Azad AF. 2015. Secretome of obligate intracellular Rickettsia. FEMS Microbiol Rev 39:47–80. https://doi.org/10.1111/1574-6976.12084.
20. Beare PA, Jeffrey BM, Long CM, Martens CM, Heinzen RA. 2018. Genetic mechanisms of Coxiella burnetii lipopolysaccharide phase variation. PLoS Pathog 14:e1006922. https://doi.org/10.1371/journal.ppat.1006922.
21. Vishwanath S. 1991. Antigenic relationships among the rickettsiae of the spotted fever and typhus groups. FEMS Microbiol Lett 65:341–344. https://doi.org/10.1111/j.1574-6968.1991.tb04783.x.
22. Needham BD, Trent MS. 2013. Fortifying the barrier: the impact of lipid A remodelling on bacterial pathogenesis. Nat Rev Microbiol 11:467–481. https://doi.org/10.1038/nrmicro3047.
23. Shi J, Zhao Y, Wang Y, Gao W, Ding J, Li P, Hu L, Shao F. 2014. Inflammatory caspases are innate immune receptors for intracellular LPS. Nature 514:187–192. https://doi.org/10.1038/nature13683.
24. Park BS, Song DH, Kim HM, Choi B-S, Lee H, Lee J-O. 2009. The structural basis of lipopolysaccharide recognition by the TLR4-MD-2 complex. Nature 458:1191–1195. https://doi.org/10.1038/nature07830.
25. Aachoui Y, Leaf IA, Hagar JA, Fontana MF, Campos CG, Zak DE, Tan MH, Cotter PA, Vance RE, Aderem A, Miao EA. 2013. Caspase-11 protects

against bacteria that escape the vacuole. Science 339:975–978. https://doi.org/10.1126/science.1230751.
26. Jordan JM, Woods ME, Soong L, Walker DH. 2009. Rickettsiae stimulate dendritic cells through Toll-like receptor 4, leading to enhanced NK cell activation in vivo. J Infect Dis 199:236–242. https://doi.org/10.1086/595833.
27. Jordan JM, Woods ME, Olano J, Walker DH. 2008. The absence of Toll-like receptor 4 signaling in C3H/HeJ mice predisposes them to overwhelming rickettsial infection and decreased protective Th1 responses. Infect Immun 76:3717–3724. https://doi.org/10.1128/IAI.00311-08.
28. Feng H-M, Whitworth T, Olano JP, Popov VL, Walker DH. 2004. Fc-dependent polyclonal antibodies and antibodies to outer membrane proteins A and B, but not to lipopolysaccharide, protect SCID mice against fatal Rickettsia conorii infection. Infect Immun 72:2222–2228. https://doi.org/10.1128/IAI.72.4.2222-2228.2004.
29. Amano K, Fujita M, Suto T. 1993. Chemical properties of lipopolysaccharides from spotted fever group rickettsiae and their common antigenicity with lipopolysaccharides from Proteus species. Infect Immun 61:4350–4355.
30. Fodorová M, Vadovič P, Toman R. 2011. Structural features of lipid A of Rickettsia typhi. Acta Virol 55:31–44. https://doi.org/10.4149/av_2011_01_31.
31. Rubin EJ, O'Brien JP, Ivanov PL, Brodbelt JS, Trent MS. 2014. Identification of a broad family of lipid A late acyltransferases with non-canonical substrate specificity. Mol Microbiol 91:887–899. https://doi.org/10.1111/mmi.12501.
32. Clementz T, Bednarski JJ, Raetz CR. 1996. Function of the *htrB* high temperature requirement gene of Escherichia coli in the acylation of lipid A: HtrB catalyzed incorporation of laurate. J Biol Chem 271:12095–12102. https://doi.org/10.1074/jbc.271.20.12095.
33. Clementz T, Zhou Z, Raetz CR. 1997. Function of the Escherichia coli msbB gene, a multicopy suppressor of htrB knockouts, in the acylation of lipid A. Acylation by MsbB follows laurate incorporation by HtrB. J Biol Chem 272:10353–10360.
34. Karow M, Georgopoulos C. 1992. Isolation and characterization of the Escherichia coli msbB gene, a multicopy suppressor of null mutations in the high-temperature requirement gene *htrB*. J Bacteriol 174:702–710. https://doi.org/10.1128/jb.174.3.702-710.1992.
35. Vorachek-Warren MK, Ramirez S, Cotter RJ, Raetz CRH. 2002. A triple mutant of Escherichia coli lacking secondary acyl chains on lipid A. J Biol Chem 277:14194–14205. https://doi.org/10.1074/jbc.M200409200.
36. Heath RJ, Rock CO. 1998. A conserved histidine is essential for glycerolipid acyltransferase catalysis. J Bacteriol 180:1425–1430.
37. Albesa-Jové D, Svetlíková Z, Tersa M, Sancho-Vaello E, Carreras-González A, Bonnet P, Arrasate P, Eguskiza A, Angala SK, Cifuente JO, Korduláková J, Jackson M, Mikušová K, Guerin ME. 2016. Structural basis for selective recognition of acyl chains by the membrane-associated acyltransferase PatA. Nat Commun 7:10906. https://doi.org/10.1038/ncomms10906.
38. White SW, Zheng J, Zhang Y-M, Rock CO. 2005. The structural biology of type II fatty acid biosynthesis. Annu Rev Biochem 74:791–831. https://doi.org/10.1146/annurev.biochem.74.082803.133524.
39. Bainbridge BW, Karimi-Naser L, Reife R, Blethen F, Ernst RK, Darveau RP. 2008. Acyl chain specificity of the acyltransferases LpxA and LpxD and substrate availability contribute to lipid A fatty acid heterogeneity in Porphyromonas gingivalis. J Bacteriol 190:4549–4558. https://doi.org/10.1128/JB.00234-08.
40. Belunis CJ, Clementz T, Carty SM, Raetz CR. 1995. Inhibition of lipopolysaccharide biosynthesis and cell growth following inactivation of the kdtA gene in Escherichia coli. J Biol Chem 270:27646–27652. https://doi.org/10.1074/jbc.270.46.27646.
41. Tersa M, Raich L, Albesa-Jové D, Trastoy B, Prandi J, Gilleron M, Rovira C, Guerin ME. 2018. The molecular mechanism of substrate recognition and catalysis of the membrane acyltransferase PatA from mycobacteria. ACS Chem Biol 13:131–140. https://doi.org/10.1021/acschembio.7b00578.
42. Dovala D, Rath CM, Hu Q, Sawyer WS, Shia S, Elling RA, Knapp MS, Metzger LE. 2016. Structure-guided enzymology of the lipid A acyltransferase LpxM reveals a dual activity mechanism. Proc Natl Acad Sci U S A 113:E6064–E6071. https://doi.org/10.1073/pnas.1610746113.
43. Turnbull AP, Rafferty JB, Sedelnikova SE, Slabas AR, Schierer TP, Kroon JT, Simon JW, Fawcett T, Nishida I, Murata N, Rice DW. 2001. Analysis of the structure, substrate specificity, and mechanism of squash glycerol-3-phosphate (1)-acyltransferase. Structure 9:347–353. https://doi.org/10.1016/S0969-2126(01)00595-0.
44. Robertson RM, Yao J, Gajewski S, Kumar G, Martin EW, Rock CO, White SW. 2017. A two-helix motif positions the lysophosphatidic acid acyltransferase active site for catalysis within the membrane bilayer. Nat Struct Mol Biol 24:666–671. https://doi.org/10.1038/nsmb.3436.
45. Scott AJ, Oyler BL, Goodlett DR, Ernst RK. 2017. Lipid A structural modifications in extreme conditions and identification of unique modifying enzymes to define the Toll-like receptor 4 structure-activity relationship. Biochim Biophys Acta 1862:1439–1450. https://doi.org/10.1016/j.bbalip.2017.01.004.
46. Kanistanon D, Hajjar AM, Pelletier MR, Gallagher LA, Kalhorn T, Shaffer SA, Goodlett DR, Rohmer L, Brittnacher MJ, Skerrett SJ, Ernst RK. 2008. A Francisella mutant in lipid a carbohydrate modification elicits protective immunity. PLoS Pathog 4:e24. https://doi.org/10.1371/journal.ppat.0040024.
47. Chandler CE, Ernst RK. 2017. Bacterial lipids: powerful modifiers of the innate immune response. F1000Res 6:1334. https://doi.org/10.12688/f1000research.11388.1.
48. Jordan JM, Woods ME, Feng H-M, Soong L, Walker DH. 2007. Rickettsiae-stimulated dendritic cells mediate protection against lethal rickettsial challenge in an animal model of spotted fever rickettsiosis. J Infect Dis 196:629–638. https://doi.org/10.1086/519686.
49. Shirey KA, Lai W, Scott AJ, Lipsky M, Mistry P, Pletneva LM, Karp CL, McAlees J, Gioannini TL, Weiss J, Chen WH, Ernst RK, Rossignol DP, Gusovsky F, Blanco JCG, Vogel SN. 2013. The TLR4 antagonist Eritoran protects mice from lethal influenza infection. Nature 497:498–502. https://doi.org/10.1038/nature12118.
50. Lina TT, Dunphy PS, Luo T, McBride JW. 2016. *Ehrlichia chaffeensis* TRP120 activates canonical Notch signaling to downregulate TLR2/4 expression and promote intracellular survival. mBio 7:e00672-16. https://doi.org/10.1128/mBio.00672-16.
51. Arias MA, Santiago L, Costas-Ramon S, Jaime-Sánchez P, Freudenberg M, Jiménez De Bagüés MP, Pardo J. 2016. Toll-like receptors 2 and 4 cooperate in the control of the emerging pathogen Brucella microti. Front Cell Infect Microbiol 6:205. https://doi.org/10.3389/fcimb.2016.00205.
52. Verhoeve VI, Jirakanwisal K, Utsuki T, Macaluso KR. 2016. Differential rickettsial transcription in bloodfeeding and non-bloodfeeding arthropod hosts. PLoS One 11:e0163769. https://doi.org/10.1371/journal.pone.0163769.
53. Rennoll SA, Rennoll-Bankert KE, Guillotte ML, Lehman SS, Driscoll TP, Beier-Sexton M, Sayeedur Rahman M, Gillespie JJ, Azad AF. 2018. The cat flea (*Ctenocephalides felis*) immune deficiency signaling pathway regulates Rickettsia typhi infection. Infect Immun 86:e00562-17. https://doi.org/10.1128/IAI.00562-17.
54. El Hamidi A, Tirsoaga A, Novikov A, Hussein A, Caroff M. 2005. Microextraction of bacterial lipid A: easy and rapid method for mass spectrometric characterization. J Lipid Res 46:1773–1778. https://doi.org/10.1194/jlr.D500014-JLR200.
55. Scott AJ, Flinders B, Cappell J, Liang T, Pelc RS, Tran B, Kilgour DPA, Heeren RMA, Goodlett DR, Ernst RK. 2016. Norharmane matrix enhances detection of endotoxin by MALDI-MS for simultaneous profiling of pathogen, host and vector systems. Pathog Dis 74:ftw097. https://doi.org/10.1093/femspd/ftw097.
56. Hittle LE, Powell DA, Jones JW, Tofigh M, Goodlett DR, Moskowitz SM, Ernst RK. 2015. Site-specific activity of the acyltransferases HtrB1 and HtrB2 in Pseudomonas aeruginosa lipid A biosynthesis. Pathog Dis 73:ftv053. https://doi.org/10.1093/femspd/ftv053.
57. Crooks GE, Hon G, Chandonia J-M, Brenner SE. 2004. WebLogo: a sequence logo generator. Genome Res 14:1188–1190. https://doi.org/10.1101/gr.849004.
58. Kelley LA, Sternberg MJE. 2009. Protein structure prediction on the Web: a case study using the Phyre server. Nat Protoc 4:363–371. https://doi.org/10.1038/nprot.2009.2.
59. Yao J, Rock CO. 2013. Phosphatidic acid synthesis in bacteria. Biochim Biophys Acta 1831:495–502. https://doi.org/10.1016/j.bbalip.2012.08.018.
60. Lewin TM, Wang P, Coleman RA. 1999. Analysis of amino acid motifs diagnostic for the *sn*-glycerol-3-phosphate acyltransferase reaction. Biochemistry 38:5764–5771. https://doi.org/10.1021/bi982805d.
61. Neuwald AF. 1997. Barth syndrome may be due to an acyltransferase deficiency. Curr Biol 7:R465–R466. https://doi.org/10.1016/S0960-9822(06)00237-5.